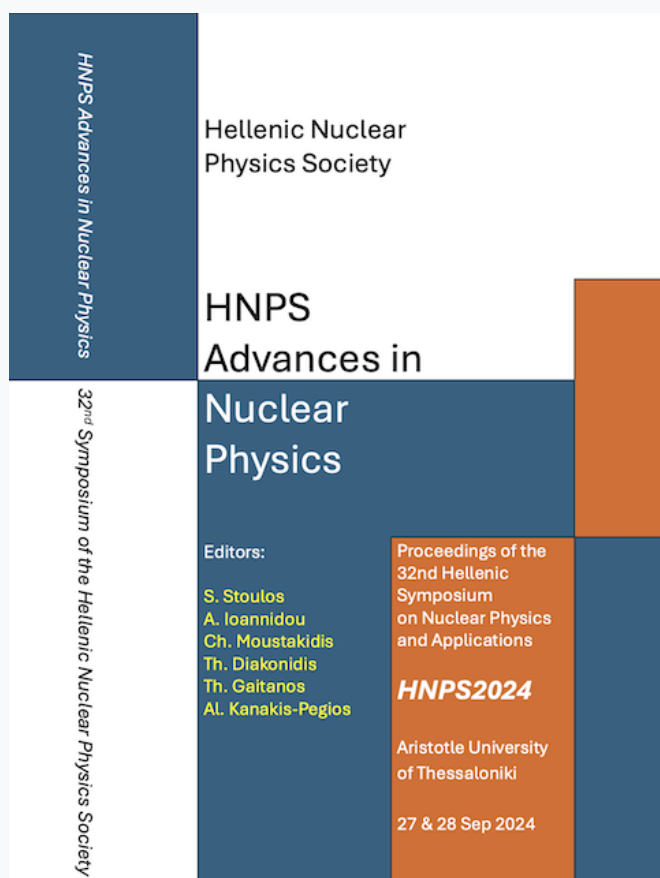


# HNPS Advances in Nuclear Physics

Vol 31 (2025)

HNPS2024



The cover image features a blue and orange color scheme. On the left, a vertical blue bar contains the text "HNPS Advances in Nuclear Physics" and "32nd Symposium of the Hellenic Nuclear Physics Society". The main title "HNPS Advances in Nuclear Physics" is prominently displayed in the center. Below the title, the editors' names are listed: S. Stoulos, A. Ioannidou, Ch. Moustakidis, Th. Diakonidis, Th. Gaitanos, and Al. Kanakis-Pegios. To the right of the editors' names, it states "Proceedings of the 32nd Hellenic Symposium on Nuclear Physics and Applications", "HNPS2024", and "Aristotle University of Thessaloniki, 27 & 28 Sep 2024".

## Atmospheric neutron measurements with Spherical Proportional Counter and the wall effect problem

*Ioanna Goula, Ilias Savvidis*

doi: [10.12681/hnpsanp.7885](https://doi.org/10.12681/hnpsanp.7885)

Copyright © 2025, Ioanna Goula, Ilias Savvidis



This work is licensed under a [Creative Commons Attribution-NonCommercial-NoDerivatives 4.0](https://creativecommons.org/licenses/by-nc-nd/4.0/).

### To cite this article:

Goula, I., & Ilias Savvidis. (2025). Atmospheric neutron measurements with Spherical Proportional Counter and the wall effect problem. *HNPS Advances in Nuclear Physics*, 31, 34–40. <https://doi.org/10.12681/hnpsanp.7885>

# Atmospheric neutron measurements with Spherical Proportional Counter and the wall effect problem

I. Goula\* and I. Savvidis

Aristotle University of Thessaloniki, 54124, Thessaloniki, Greece

**Abstract** Cosmic radiation interacts with molecules, atoms and nuclei in the atmosphere producing secondary radiation consisting of charged particles, neutrons, gamma and X-rays. The cosmic neutron energy ranges from 0.01eV to 10GeV, with neutrons of low energy being difficult to detect and measure. The Spherical Proportional Counter (SPC) is a large-volume gaseous detector and has been optimized for operation with pure nitrogen gas to be used for detection of thermal neutrons via the  $^{14}\text{N}(n,p)^{14}\text{C}$  reaction. When the reaction happens close to the detector wall it is possible for the produced particles to hit the wall and lose energy. This is known as the wall effect, and it leads to wrong calculations of the incident particle energy. The challenge for thermal neutron detection lies in achieving sufficient gas gain since low pressure is needed which results in non-negligible wall effect [3]. In this work, a study has been done to quantify the wall effect of thermal neutrons in the SPC. We used GEANT4 simulations to produce neutron beams that cover the total volume of the sphere interacting with the gas nuclei and then analyzed the data using python code.

**Keywords** atmospheric neutrons, Spherical Proportional Counter, wall effect

## INTRODUCTION

### Atmospheric neutrons

Atmospheric neutrons are all generated by the interaction of the cosmic rays with oxygen and nitrogen nuclei that exist in the air (Fig. 1). The primary cosmic rays consist of 85% protons, 13% alpha and 2% heavier particles with  $Z > 2$ . There is no evidence indicating any neutron flux in the primary radiation and because of the short half-life it is unlikely that neutrons could reach the Earth from regions more distant than the Sun [1].

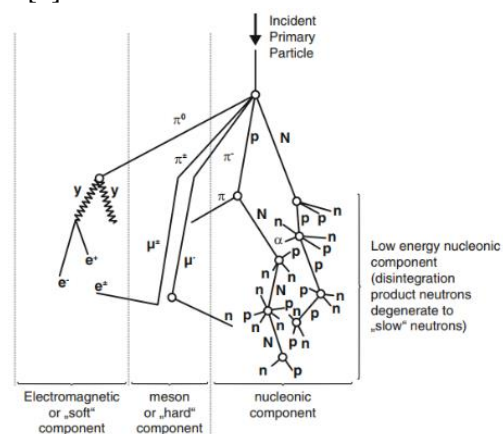


**Figure 1.** Production of neutrons from cosmic ray interactions [2]

### Cosmic rays and neutron flux

Since atmospheric neutrons are produced by cosmic rays the factors that affect the rays flux also affect the flux of neutrons.

\* Corresponding author: igoula@physics.auth.gr

Solar cosmic rays are produced during solar flares in which several GeV-charged particles are ejected as solar wind, whose intensity changes during the 11-year solar activity cycle. When solar activity is high, the solar wind is stronger and so are the magnetic fields it carries, resulting in a decrease of the cosmic ray flux.

To enter the atmosphere, cosmic rays must penetrate the magnetic field. This ability is called magnetic rigidity and for each point it takes a value called geomagnetic cutoff below which rays cannot arrive. The cutoff is lower near the poles, so the intensity of cosmic radiation is larger at higher latitudes decreasing as we approach the equator line.

Also, the atmosphere provides shielding against cosmic rays which at a given altitude is determined by the atmosphere depth. The higher the altitude, the higher the flux of cosmic rays [3].

### *Atmospheric neutron spectra*

The majority of high energy neutrons are produced in hadronic air showers by charge-exchange interactions between cosmic rays and atmospheric nuclei. This results in neutrons with energies exceeding 1 GeV.

Neutrons in the sub-GeV region are also produced in these air showers, through head-on collisions of cosmic rays with atmospheric nucleons. In the collision a nucleon gains momentum inside the nucleus and forms an intranuclear cascade resulting in neutrons with 10's to 100's of MeV energy.

The produced cascade is followed by the emission of particles from the excited remnant nucleus. This process is called evaporation, the nucleus moves to its ground state by emitting photons and hadrons, including neutrons with energies around 1 MeV.

After production, neutrons lose energy by scattering off of atmospheric nuclei in a process called thermalization [4].

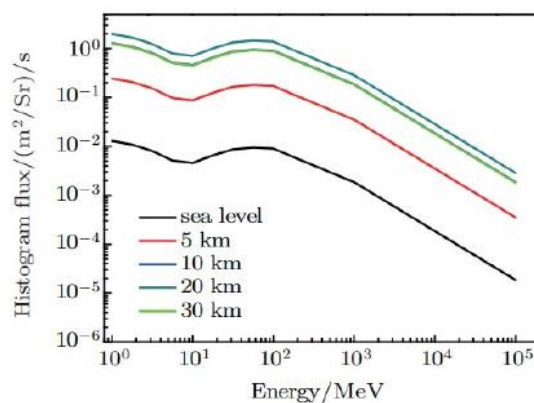


**Figure 2.** Atmospheric neutron spectrum at different altitudes [5]

### *Motivation*

In our study we will be focusing on atmospheric thermal neutrons. These neutrons can cause single event upsets in the experiments resulting in an unavoidable background. The neutron-induced background cannot be reduced through active shielding due to the non-ionizing behavior of neutrons, while passive shielding results in a significant mass increase of the payload. It is clear that we need to understand the neutron flux to optimize our experiments.

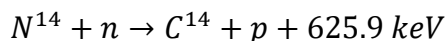
## **EXPERIMENTAL DETAILS**

### *The wall effect and the detection reaction*

In order to detect and measure the energy of an incoming particle it is important to deposit all its

energy inside the sensitive volume of the detector. However, when a reaction happens close to the vessel wall or the range of the particle is large, there is a possibility that it will hit the wall and lose energy. This phenomenon is called wall effect and can lead to wrong estimations [6].

To measure and quantify the wall effect we use the (n,p) reaction in nitrogen gas, which has a significant cross section for thermal neutrons.



The energy is split between the products with the mean energy of carbon being  $\approx 42 \text{ keV}$  and for proton  $\approx 584 \text{ keV}$ .

### The detector

The large Spherical Proportional Counter is a gaseous detector [7] consisting of a spherical copper shell with 6mm thickness and 130cm diameter placed at ground level (see Fig. 3).

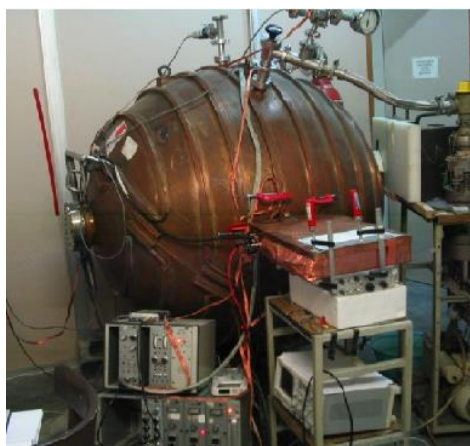


**Figure 3.** The Spherical Proportional Counter of the lab at Aristotle University

In Figure 4 we see the wall effect of the particles as a function of their range inside the small SPC with a 30 cm diameter for 1 bar, as it has been determined in our previous work [8]. From the reactions of thermal neutrons -despite their small energy- we expect protons with a range close to 5 cm, which corresponds to  $\approx 20\%$  of the events to be lost due to wall effect. So, it becomes clear that the small SPC is not a suitable detector for the study that we want to perform, that is the reason why we are moving to the larger one.

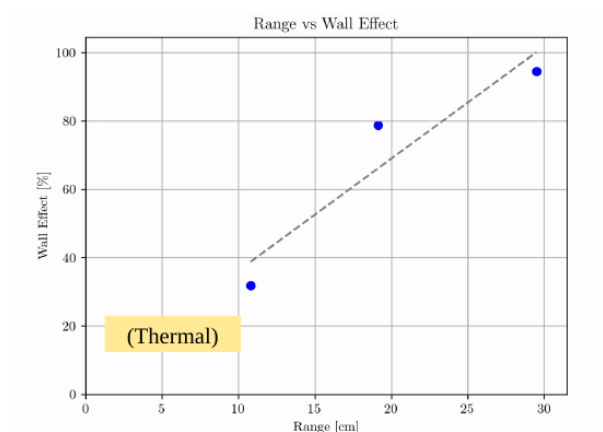


**Figure 4.** Wall effect as a function of particles range for SPC ( $\Phi=30\text{cm}$ ) at 1 bar

### The simulation

In our work, to study the atmospheric thermal neutrons and the wall effect inside the SPC we

used GEANT4, a Monte-Carlo based simulation framework [9]. The simulation was built based on the “Hadr06” example from the provided files with modifications to correspond to our specific detector geometry and gas.

We simulated the SPC of the lab, filled with nitrogen gas in two cases, 1 bar pressure and 200 mbar pressure. The simulated neutron beams consist of 5’000’000 thermal neutrons with 0.025 eV energy for each run, isotropically incident on the detector.

The analysis of the data was performed using python code. We calculated the total energy deposition from the neutrons and counted the total number of (n,p) reactions. Then, we calculated the percentage of produced particles that hit the wall and registered them as lost due to wall effect.

## RESULTS AND DISCUSSION

### Results for 1 bar

We detected the (n,p) reactions first for 1bar pressure and measured the energy of the protons and carbon at the moment of their creation, which when looking at the histograms (Fig. 5) seem to be in very good agreement with literature.

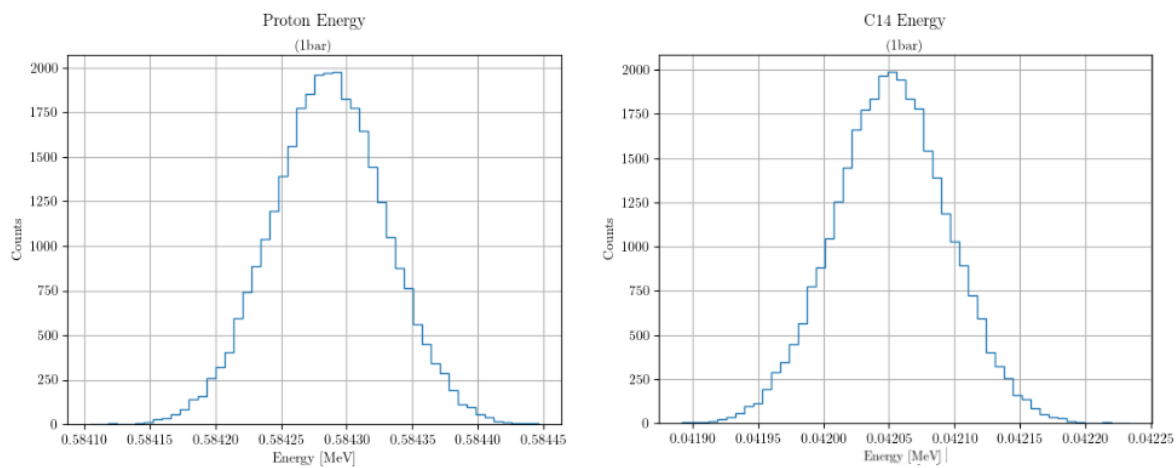


**Figure 5.** Proton (left) and carbon (right) energy at creation for 1 bar.

We also plotted the histogram (Fig. 6) for the total energy deposited by thermal neutrons inside the nitrogen gas. The clear, narrow peak at 0.7 MeV corresponds to the (n,p) reaction, while the one on its left forms when neutrons interact inside the copper shell upon entry and the produced particles enter and ionize the gas.

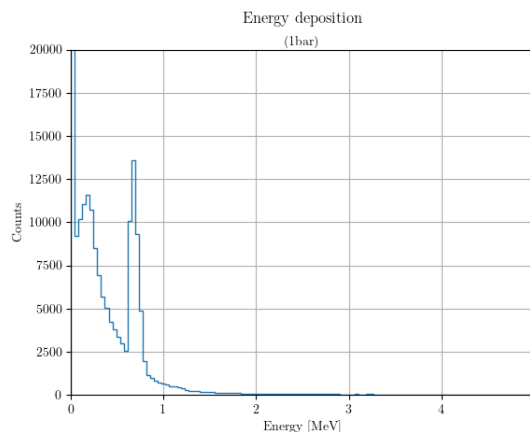


**Figure 6.** Total energy deposition in the nitrogen gas for 1 bar.

In the case of 1 bar, we analyzed the simulated data and found the wall effect percentage  $\approx 0.898\%$ , which can almost be considered negligible.

### Results for 200 mbar

For the case of 200 mbar, we followed the same procedure (Fig. 7) and observing the proton and carbon histogram we find that the energy is split again in the expected way.

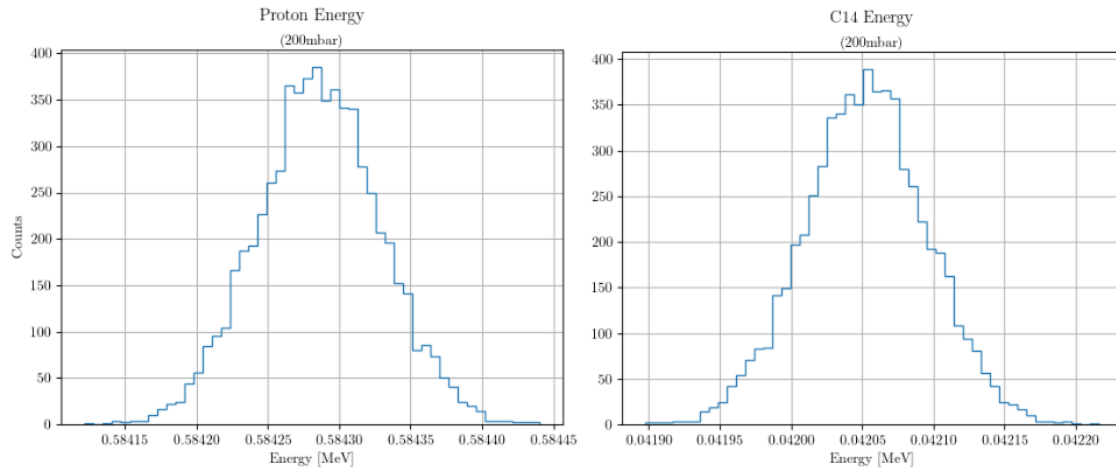


**Figure 7.** Proton (left) and carbon (right) energy at creation for 200 mbar.

In the total energy deposition histogram (Fig. 8), we can distinguish the (n,p) detection peak close to 0.7 MeV clearly, though not as clear as the case of 1 bar. Analyzing the 200-mbar data the wall effect percentage was found to be  $\approx 4.458\%$ , which is not very high and allows the large SPC to be used at low pressure for thermal neutron studies.

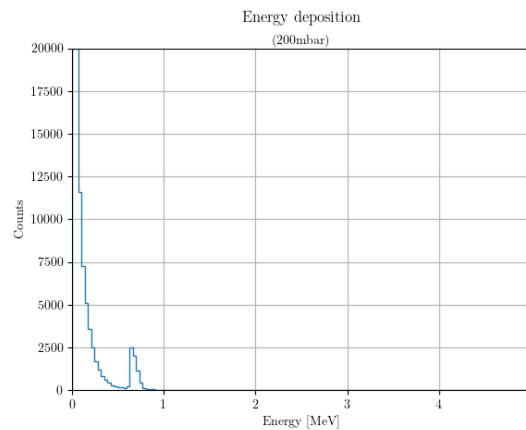


**Figure 8.** Total energy deposition in the nitrogen gas for 200 mbar.

### Experimental results for 200 mbar

An  $^{241}\text{Am}$  alpha source has been used to calibrate the detector, and the figures can be helpful to recognize the shape of the signal that is expected from the detection of thermal neutrons (Fig. 9). After calibration the alpha source was removed, and the detector was irradiated by atmospheric neutrons at 200 mbar pressure.

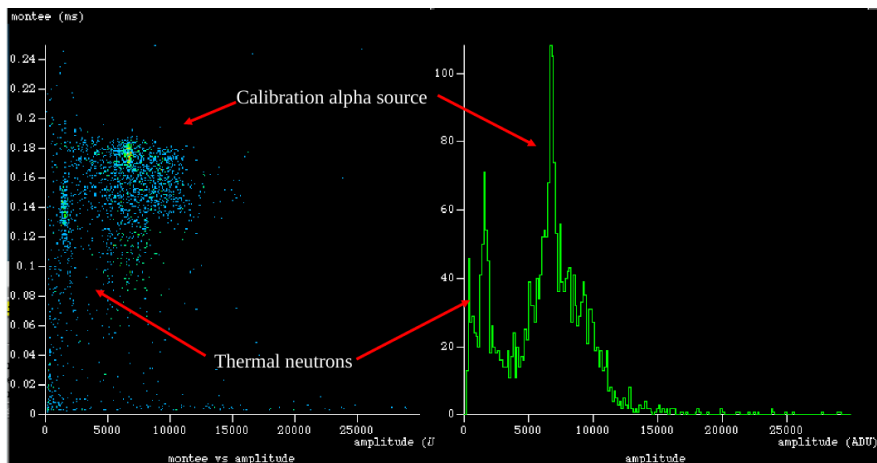


**Figure 9.** Calibration of the detector

It can be seen from the amplitude histograms that two peaks are formed (Fig. 10). By looking at the risetime-amplitude plot we understand that the small peak at 2000ADU corresponds to thermal neutrons, while the broad peak on the right forms due to background radiation that can be eliminated, however requires a very complicated process.

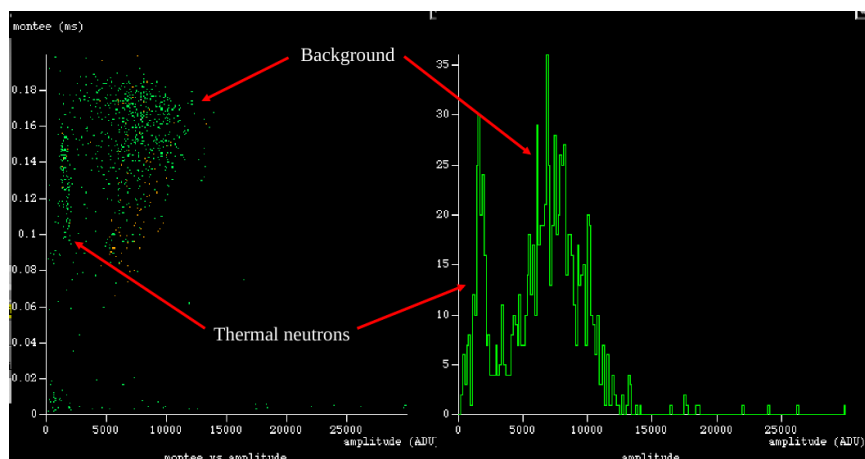


**Figure 10.** Experimental measurements of thermal neutrons for 200 mbar

## CONCLUSIONS

In our study it has been shown both with simulations and experiments that the large Spherical Proportional Counter can be used to detect and measure the atmospheric thermal neutrons. This is important not only for improving the experiments by reducing the background, but also for practical applications, such as evaluating radiation risks in different environments.

## References

- [1] W.N. Hess, et al., Phys. Rev. 116, 445 (1959); doi: 10.1103/PhysRev.116.445
- [2] J. Beer, et al., "Production of Cosmogenic Radionuclides in the Atmosphere", In: Cosmogenic Radionuclides. Physics of Earth and Space Environments. Springer, Berlin, Heidelberg, 139, (2011); doi: 10.1007/978-3-642-14651-0\_10
- [3] H.R. Vega-Carrillo, et al., "Study of the environmental neutron spectrum at Zacatecas city" in National Congress on Solid State Dosimetry, Mexico (2003)
- [4] M. Kole, et al., Astropart. Phys. 62, 230 (2015); doi: 10.1016/j.astropartphys.2014.10.002
- [5] Zhi-Feng Lei, et al., Chin. Phys. B 27, 066105 (2018); doi: 10.1088/1674-1056/27/6/066105



- [6] E. Bougamont, et al., *Nucl. Instrum. Meth. Phys. Res. A* 847, 10 (2017); doi: 10.1016/j.nima.2016.11.007
- [7] I. Giomataris, et al., *JINST* 3, 09007 (2008); doi: 10.1088/1748-0221/3/09/P09007
- [8] I. Goula, et al., *HNPS Adv. Nucl. Phys.* 30, 110 (2024); doi: 10.12681/hnpsanp.6250
- [9] S. Agostinelli, et al., *Nucl. Instrum. Meth. Phys. Res. A* 506, 250 (2003); doi: 10.1016/S0168-9002(03)01368-8